

# Targeting PKC in multiple myeloma: in vitro and in vivo effects of the novel, orally available small-molecule inhibitor enzastaurin (LY317615.HCl)

Klaus Podar,<sup>1</sup> Marc S. Raab,<sup>1-2</sup> Jing Zhang,<sup>1</sup> Douglas McMillin,<sup>1</sup> Iris Breitskreutz,<sup>1</sup> Yu-Tzu Tai,<sup>1</sup> Boris K. Lin,<sup>3</sup> Nikhil Munshi,<sup>1</sup> Teru Hideshima,<sup>1</sup> Dharminder Chauhan,<sup>1</sup> and Kenneth C. Anderson<sup>1</sup>

<sup>1</sup>Department of Medical Oncology, Dana-Farber Cancer Institute, Harvard Medical School, Boston, MA; <sup>2</sup>Department of Internal Medicine V, University of Heidelberg, Germany; and <sup>3</sup>Eli Lilly and Company, Indianapolis, IN

**In multiple myeloma (MM) protein kinase C (PKC) signaling pathways have been implicated in cell proliferation, survival, and migration. Here we investigated the novel, orally available PKC-inhibitor enzastaurin for its anti-MM activity. Enzastaurin specifically inhibits phorbol ester-induced activation of PKC isoforms, as well as phosphorylation of downstream signaling molecules MARCKS and PKC $\mu$ . Importantly, it also inhibits PKC activation triggered by growth factors and cytokines secreted by bone marrow stromal**

**cells (BMSCs), costimulation with fibronectin, vascular endothelial growth factor (VEGF), or interleukin-6 (IL-6), as well as MM patient serum. Consequently, enzastaurin inhibits proliferation, survival, and migration of MM cell lines and MM cells isolated from multidrug-resistant patients and overcomes MM-cell growth triggered by binding to BMSCs and endothelial cells. Importantly, strong synergistic cytotoxicity is observed when enzastaurin is combined with bortezomib and moderate synergistic or additive ef-**

**fects when combined with melphalan or lenalidomide. Finally, tumor growth, survival, and angiogenesis are abrogated by enzastaurin in an in vivo xenograft model of human MM. Our results therefore demonstrate in vitro and in vivo efficacy of the orally available PKC inhibitor enzastaurin in MM and strongly support its clinical evaluation, alone or in combination therapies, to improve outcome in patients with MM. (Blood. 2007;109:1669-1677)**

© 2007 by The American Society of Hematology

## Introduction

Characterized by clonal proliferation of immunoglobulin-secreting plasma cells within the bone marrow (BM), multiple myeloma (MM) is the most common hematologic malignancy in patients older than 65 years. Although conventional and novel therapies such as thalidomide, bortezomib, and lenalidomide have prolonged progression-free and overall survival, MM remains incurable. The delineation of signaling pathways, which mediate MM-cell growth, survival, and migration within the BM microenvironment, can both enhance our understanding of disease pathogenesis and identify molecular targets for novel MM therapies to improve patient outcome.

The PKC family of serine/threonine kinases is comprised of at least 12 isoforms, which are classified into 3 structurally and functionally distinct subgroups: conventional isoforms (cPKC including PKC $\alpha$ , PKC $\beta$ I, PKC $\beta$ II, PKC $\gamma$ ); novel isoforms (nPKC including PKC $\delta$ , PKC $\epsilon$ , PKC $\eta$ , PKC $\theta$ ); and atypical isoforms (aPKC including PKC $\zeta$ , PKC $\lambda$ / $\iota$ ). Based on homology within the catalytic domain, PKC $\mu$ /PKD and PKC $\nu$  were recently added to the PKC superfamily. PKC isoforms show tissue- and cell-type-specific expression and function<sup>1</sup> and have been implicated in the regulation of cell growth, differentiation, apoptosis, cytokine secretion, migration, and membrane permeability during tumorigenesis.<sup>2-7</sup> Phorbol esters (phorbol-12-myristate-13-acetate [PMA] or 12-O-tetradecanoylphorbol 13-acetate [TPA]) are powerful tumor promoters,<sup>8</sup> and PKC is the major cellular phorbol-ester receptor.<sup>9-11</sup> Specifically, similar to DAG, phorbol esters increase PKC-binding affinity to the plasma-cell membrane by serving as

hydrophobic anchors and also stabilize the active PKC conformation. Importantly, increased levels of PKC are observed in breast, lung, and gastric carcinomas; during early colon carcinogenesis; and in malignant gliomas.<sup>12-16</sup> Conversely, inhibition of PKC abrogates tumor growth in xenograft mouse models of bladder, lung, and colon carcinoma.<sup>17</sup> Besides solid tumors, members of the PKC family have also been implicated in hematologic malignancies: overexpression of PKC $\beta$  has been reported in patients with progressive diffuse large B-cell lymphoma (DLBCL)<sup>18,19</sup> as well as T-cell lymphomas and T-cell leukemias.<sup>20-22</sup> In addition to their direct tumorigenic sequelae within tumor cells, PKC signaling pathways are also intimately linked to tumor-induced and TPA-induced angiogenesis.<sup>23,24</sup>

Given its proposed key role in tumorigenesis, PKC is a promising new target in cancer therapy. The macrocyclic bisindolylmaleimide enzastaurin (LY317615.HCl) is a novel orally available PKC inhibitor. Enzastaurin competes with ATP for the nucleotide triphosphate-binding site of PKC, thereby blocking its activation. Besides its major target PKC $\beta$ , enzastaurin also potently inhibits other PKC isoforms including PKC $\delta$ , PKC $\epsilon$ , PKC $\gamma$ , and PKC $\alpha$ .<sup>25</sup> Although enzastaurin was initially developed for antiangiogenic cancer therapy,<sup>26</sup> recent preclinical studies demonstrate significant antitumor activity against cell lines of colon cancer (HCT116), glioblastoma (U87MG), prostate cancer (PC-3), cutaneous T-cell lymphoma (HH, HuT-78), leukemia (K562 and MOLT-4), and non-small-cell cancer (HOP-92).<sup>25,27</sup> Early clinical studies show that enzastaurin is well tolerated within a dosage range of 20 to 700

Submitted August 24, 2006; accepted September 25, 2006. Prepublished online as *Blood* First Edition Paper, October 5, 2006; DOI 10.1182/blood-2006-08-042747.

The online version of this article contains a data supplement.

The publication costs of this article were defrayed in part by page charge payment. Therefore, and solely to indicate this fact, this article is hereby marked "advertisement" in accordance with 18 USC section 1734.

© 2007 by The American Society of Hematology

mg/d, without reaching a maximally tolerated dose. Mean steady-state plasma levels of 2  $\mu$ M were achieved after oral administration of 525 mg/d enzastaurin.<sup>28</sup> Several clinical trials are now ongoing to test enzastaurin in a variety of malignancies including recurrent brain tumor (phase 1), advanced or metastatic malignancies (phase 2), advanced non-small-cell lung cancer (NSCLC; phase 2), metastatic colorectal cancer (phase 2), advanced or metastatic pancreatic cancer, combined with gemcitabine (phase 2), and glioblastoma multiforme (phase 3), and for prevention of relapse in DLBCL (phase 3; www.clinicaltrials.gov).

In MM, PKC isoform expression has been reported in several MM cell lines.<sup>29-33</sup> Functionally, PKCs are: (1) involved in MM-cell apoptosis<sup>30,34</sup>; (2) required for VEGF- and Wnt-induced MM-cell migration<sup>33,35</sup>; and (3) associated with the control of IL-6 receptor- $\alpha$  shedding.<sup>31</sup> Importantly, the unique gene signature of MM patients with the adverse prognostic t(4;14)(p16;q32) translocation shows marked up-regulation of PKC $\beta$ .<sup>36,37</sup> Taken together, these data suggest an important role of PKC in MM pathogenesis. However, whether the novel PKC inhibitor enzastaurin is active in MM is unknown. In this study, we show that its cytotoxicity against MM both in vitro and in vivo strongly supports its clinical evaluation, alone or in combination with other novel or conventional therapies to improve outcome in patients with MM.

## Materials and methods

### Materials

Enzastaurin (LY317615.HCl) was provided by Eli Lilly (Lilly Research Labs, Eli Lilly and Company, Indianapolis, IN). Other reagents were obtained as follows: VEGF<sub>165</sub> from R&D Systems (Minneapolis, MN); TPA (12-O-tetradecanoyl-phorbol-13-acetate); pPKC(Thr638/641), pPKC(Ser660), pPKC $\delta$ (Thr505), and pMARCKS antibodies from Cell Signaling Technology (Beverly, MA); pERK, ERK-2, caspase-8, PARP, Mcl-1, Bcl-2, Bcl-XL, and nucleolin antibodies from Santa Cruz Biotechnology (Santa Cruz, CA); and PKC $\alpha$ , PKC $\beta$ , PKC $\gamma$ , PKC $\epsilon$  antibodies from BD Biosciences-PharMingen (San Diego, CA). Specifically, phospho-antibodies are directed against the PKC isoform residues homologous to the activation loop Thr-514 of PKC $\gamma$  (PKC $\alpha$ , PKC $\beta$ , PKC $\gamma$ , PKC $\delta$ , PKC $\epsilon$ , PKC $\eta$ , PKC $\theta$ ), to the regulatory Ser-660 of PKC $\beta$ II (PKC $\alpha$ , PKC $\beta$ , PKC $\delta$ , PKC $\epsilon$ , and PKC $\eta$ ), and the regulatory Thr-638/641 (PKC $\alpha$ , PKC $\beta$ ).

### Cells and cell culture

All human MM cell lines and primary patient MM cells were cultured as previously described.<sup>32</sup> Human umbilical vein endothelial cells (HUVECs) from a pool of 5 healthy donors (kindly provided by Drs A. Cardoso and M. Tavares, Dana-Farber Cancer Institute [DFCI]) were maintained in EGM-2MV media (Clonetics BioWhittaker, Walkersville, MD) containing 2% FBS.

### Isolation of patient tumor cells

After patients provided informed consent in accordance with the Declaration of Helsinki and approval by the Institutional Review Board of the DFCI, MM patient cells (96% CD38<sup>+</sup>CD45RA<sup>-</sup>) were obtained as previously described.<sup>32</sup>

### Cell fractionation

After washing 3 times with phosphate-buffered saline, MM.1S cells were transferred into 400  $\mu$ L hypotonic lysis buffer followed by cell fractionation as previously described.<sup>32</sup>

### Cell lysis, immunoprecipitation, and Western blotting

Cell lysis, immunoprecipitation, and Western blot analysis were performed as described previously.<sup>32</sup>

### Measurement of PKC activity

PKC activity was measured with a PKC assay kit (Upstate Biotechnology, Lake Placid, NY) according to the manufacturer's instructions and as described previously.<sup>32</sup>

### DNA synthesis and cell-proliferation assay

Cell growth was assessed by measuring [<sup>3</sup>H]-thymidine uptake, as described in prior studies.<sup>32</sup>

### Cell adhesion assays

Adhesion assays were performed using the Vybrant cell-adhesion assay kit (Molecular Probes, Eugene, OR), as previously described.<sup>32</sup> All experiments were done in triplicate.

### Annexin/PI stain, SYTOX green nucleic acid stain, MTT assay

Enzastaurin in solution has an intense orange color. Besides method-related adequate baseline normalization, we therefore used a variety of apoptosis/cytotoxicity assays to confirm our results under different conditions. MM.1S cells were treated with either vehicle or enzastaurin for 24 hours and 48 hours, washed with PBS, and evaluated for annexin V (BD PharMingen) or SYTOX green nucleic acid staining (Invitrogen/Molecular Probes) using a fluorescence-activated cell sorter (FACS).

### MTT colorimetric survival assay

The inhibitory effect of enzastaurin on MM cell lines was assessed using MTT assay, as described previously.<sup>38</sup> Cell survival was estimated as a percentage of the value of untreated controls.

### Transwell migration assay

Cell migration was assayed using a modified Boyden chamber assay, as described previously.<sup>32</sup>

### In vitro angiogenesis assay

The antiangiogenic potential of enzastaurin was studied using an in vitro angiogenesis assay kit (Chemicon, Temecula, CA), as per manufacturer's instructions. Tube formation was assessed using an inverted light/fluorescence microscope at  $\times 4$  to  $\times 10$  magnification. Photographs are representative of each group and 3 independent experiments.

### Isobologram analysis

For combination studies, data from [<sup>3</sup>H][dT] uptake assays were converted into values representing the fraction of growth affected (FA) in drug-treated versus untreated cells and analyzed using CalcuSyn software program (Biosoft, Ferguson, MO) based on the Chou-Talalay method. A combination index (CI) smaller than 1 indicates synergism, whereas 0.9 to 1.1 indicates additive effects.

### MM xenograft mouse model

To determine the in vivo anti-MM activity of enzastaurin, beige-nude Xid mice were inoculated subcutaneously in the right flank with  $3 \times 10^7$  MM.1S MM cells in 100  $\mu$ L RPMI 1640 medium, together with 100  $\mu$ L Matrigel (Becton Dickinson Biosciences, Bedford, MA). When tumor was measurable, mice were assigned to the enzastaurin treatment group or a control group. Enzastaurin was dissolved in 100% ethanol, diluted 1:10 in D5W (Sigma-Aldrich, St Louis, MO), and given twice daily by oral gavage for indicated periods. The control group received the carrier alone at the same schedule and route of administration. Tumor burden was measured every alternate day using a caliper (calculated volume =  $4\pi/3 \times (\text{width}/2)^2 \times (\text{length}/2)$ ). Animals were killed when their tumor reached 2 cm or when the mice became moribund. Survival was evaluated from the first day of treatment until death. All animal studies were approved by the Dana-Farber Animal Care and Use Committee.

## Immunohistochemistry

Sections (4  $\mu\text{m}$ ) of formalin-fixed tissue were used for TUNEL staining and staining with CD31 antibody (BD PharMingen, San Diego, CA) in a humid chamber at room temperature, as in prior studies.<sup>39</sup> Leica N Plan 5 $\times$ /0.12 PH0, Leica N Plan 10 $\times$ /0.25 PH1, and Leica HCX PL Fluotar 40 $\times$ /0.60 corr PH2 XT objective lenses were used.

## Statistical analysis

Statistical significance of differences observed in enzastaurin-treated versus control-cell cultures was determined using an unpaired Student *t* test. The minimal level of significance was *P* below .05. Overall survival in animal studies was measured using the Kaplan-Meier method, and results are presented as the median overall survival, with 95% confidence intervals (CIs).

## Results

### Enzastaurin specifically inhibits TPA-triggered phosphorylation and activation of PKC isoforms in MM cells

PKC isoforms (PKC $\alpha$ , PKC $\beta$ , PKC $\delta$ , PKC $\epsilon$ , PKC $\zeta$ , PKC $\iota$ , and PKC $\mu$ ) are expressed in a large array of MM cell lines including dexamethasone-sensitive MM.1S, dexamethasone-resistant MM.1R, RPMI 8226, doxorubicin-resistant RPMI-Dox40 (Dox40), melphalan-resistant RPMI-LR5 (LR5), IL-6-dependent INA6, U266, as well as in NCI-H929 (with wild-type FGFR3 overexpression), OPM-1 and OPM-2 (with FGFR3 mutation K650E), KMS-11 (with FGFR3 mutation Y373C), and patient MM cells. Specifically, our results show overall high expression of PKC $\alpha$ , PKC $\delta$ , and PKC $\epsilon$ ; overall low expression of PKC $\beta$ , PKC $\zeta$ , PKC $\iota$ , and PKC $\mu$ ; and low expression or absence of PKC $\gamma$  and PKC $\theta$  (Table S1, available on the *Blood* website; see the Supplemental Table link at the top of the online article). Here, we therefore focus on PKC $\alpha$ , PKC $\delta$ , PKC $\epsilon$ , and PKC $\beta$ , the major targets of enzastaurin.

The PKC inhibitor enzastaurin has already demonstrated marked preclinical and early clinical activity in a variety of tumors. In MM, PKCs are required for VEGF-induced MM-cell migration in our model cell line MM.1S as well as other MM cell lines and primary MM cells.<sup>35</sup> The therapeutic potential of targeting PKC in MM has only recently been studied. Specifically, Rizvi et al showed that enzastaurin induced apoptosis in MM cell lines.<sup>40</sup> In this study we further characterize the molecular mechanism whereby enzastaurin mediates *in vitro* and *in vivo* MM cytotoxicity. Typically, cPKCs and nPKCs change their conformation on membrane recruitment, thereby enabling both enzyme activation and subsequent substrate phosphorylation. We therefore first investigated whether enzastaurin abrogates TPA-induced PKC activation in MM.1S cells using both phospho-specific antibodies as well as immunoprecipitation kinase assays. Although enzastaurin did not inhibit TPA-induced recruitment of PKC isoforms to the plasma-cell membrane, it blocked TPA-induced homologous PKC activation loop Thr-514 and carboxy-terminal Ser-660 phosphorylation within the cytoplasm, Ser-660 phosphorylation at the plasma-cell membrane, as well as Thr-514 and Ser-660 phosphorylation within the nucleus. Less impressive differences in membrane-associated phosphorylation of Thr-514 may be due to enzastaurin-induced sustained PKC binding to the plasma-cell membrane, thereby blocking release of activated PKC into the cytoplasm (Figure 1A). In contrast to Thr-514 and Ser-660 phosphorylation, constitutive phosphorylation of regulatory PKC Thr-638 or Thr-641 (pPKC $\alpha/\beta$ ) residues remained unchanged on enzastaurin treatment (data not shown). Conversely, immunoprecipitations with phospho-PKC Thr-514

(Figure 1B) and Ser-660 (Figure 1C) antibodies showed marked enzastaurin-induced inhibition of PKC $\alpha$ , PKC $\beta$ , and PKC $\epsilon$ . Despite only minor changes in regulatory Ser-643 (data not shown) and Ser-662 (homologous to Ser-660), PKC $\delta$  phosphorylation (Figure 1C, fourth panel from top) and marked down-regulation of activation loop Thr-505 PKC $\delta$  phosphorylation (Figure 1B fourth panel from top) were triggered by enzastaurin. To verify the impact of enzastaurin-induced changes in phosphorylation on kinase activity of cPKC isoforms, we next performed immunoprecipitation kinase assays. Our results show that enzastaurin induced inhibition of both TPA-induced PKC $\alpha$  (left panel) and PKC $\beta$  (right panel) kinase activity (Figure 1D). To verify the effect of enzastaurin on kinase activity of nPKC isoforms, we performed PKC $\delta$  and PKC $\epsilon$  immunoprecipitations, followed by immunoblot analysis with phospho-specific antibodies. Consistent with the data, our results show marked inhibition of catalytic Thr-505 (Figure 1E top panel) and moderate inhibition of regulatory Ser-643 (data not shown) and Ser-660 PKC $\delta$  phosphorylation (Figure 1E, middle panel) as well as marked inhibition of both catalytic Thr-566 (homologous to Thr-514; Figure 1F, top panel) and regulatory Ser-729 (homologous to Ser-660) PKC $\epsilon$  phosphorylation (Figure 1F, middle panel). Taken together, these data demonstrate that enzastaurin differentially modulates TPA-triggered phosphorylation of PKC isoforms PKC $\alpha$ , PKC $\beta$ , PKC $\delta$ , and PKC $\epsilon$ , thereby leading to marked inhibition of kinase activity.

### Enzastaurin specifically inhibits TPA-triggered phosphorylation of signaling molecules downstream of PKC

Having shown enzastaurin-mediated effects on TPA-induced PKC isoform activation, we next evaluated its effects on downstream signaling molecules. Our results demonstrate that enzastaurin inhibited TPA-induced phosphorylation of downstream PKC $\mu$ /PKD, MARCKS, GSK3 $\beta$ , JNK1/2, ERK1/2, and c-Myc, but did not inhibit phosphorylation of PDK-1, a signaling molecule upstream of PKC, which triggers activation loop phosphorylation of cPKCs and nPKCs (Figure 2A).

### Enzastaurin inhibits PKC signaling sequelae in MM cells triggered by BMSC-secreted growth factors and cytokines, costimulation with the extracellular matrix protein fibronectin, IL-6 or VEGF, as well as patient serum

Growth factors and cytokines within the BM microenvironment (ie, IL-6 and VEGF) mediate MM-cell growth, survival, and drug resistance. We therefore next tested the impact of the BM microenvironment on MM PKC signaling. Our results show that PKC $\mu$ /PKD phosphorylation is triggered by conditioned medium from the BMSC line HS-5 (Figure 2B, SN), as well as by costimulation by both fibronectin/VEGF (Figure 2B, VEGF) and fibronectin/IL-6 (Figure 2, IL-6). Conversely, enzastaurin inhibited PKC $\mu$ /PKD activation triggered by these stimuli (Figure 2B). Furthermore, serum isolated from MM patient BM strongly triggered Thr-514 phosphorylation as well as activation of downstream signaling molecules including MARCKS, JNK, and c-Myc. Conversely, treatment with enzastaurin strongly inhibited serum-induced phosphorylation of catalytic Thr-514 PKC and downstream signaling molecules (Figure 2C). Taken together, these data confirm that enzastaurin inhibits PKC activation triggered by BMSC-secreted growth factors and cytokines, costimulation with the extracellular matrix protein fibronectin, VEGF or IL-6, as well as MM patient serum.

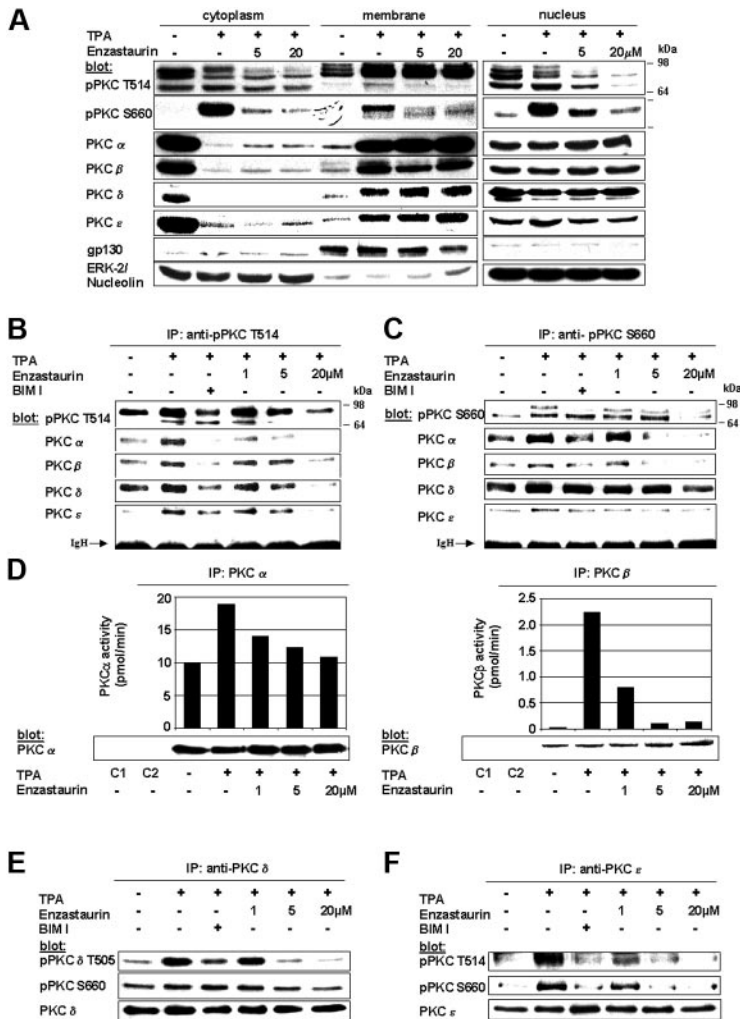


**Figure 1. Enzastaurin specifically inhibits TPA-triggered phosphorylation and activation of PKC isoforms.** (A) Enzastaurin inhibits TPA-induced phosphorylation of homologous PKC residues, but not PKC subcellular relocalization. Prior to TPA stimulation (200 nM, 20 minutes), MM.1S cells were treated with indicated concentrations of enzastaurin (3 hours) or left untreated. Immunoblots of cytosolic, membrane, and nuclear fractions were probed with indicated antibodies. The presence of gp130 in the membrane fraction and its absence in the cytosolic and nuclear fraction, as well as the presence of ERK-2 in the cytosolic and nucleolin in the nuclear fraction, served as controls for the purity of subcellular fractionation. (B-C) Enzastaurin specifically inhibits homologous Thr-514 and Ser-660 residue phosphorylation of PKC isoforms. MM.1S cells were treated with indicated concentrations of enzastaurin (3 hours), bisindolylmaleimide (BIM I, 2  $\mu$ M), or left untreated. After stimulation with TPA (200 nM, 20 minutes), equal amounts of whole-cell lysates were immunoprecipitated with pPKC antibodies directed against the catalytic Thr-514 (B) or the regulatory Ser-660 (C) residue, and then immunoblotted with the indicated antibodies. IgH indicates immunoglobulin heavy chain. (d) Enzastaurin specifically inhibits conventional PKC isoform kinase activity. PKC isoform activity was determined using PKC immunoprecipitation kinase assays, as described in "Materials and methods." (E-F) Enzastaurin specifically inhibits novel PKC isoform kinase activity. After stimulation with TPA (200 nM, 20 minutes), equal amounts of whole-cell lysates were immunoprecipitated with PKC $\delta$  (E) or PKC $\epsilon$  (F) antibodies and immunoblotted with indicated antibodies. IP indicates immunoprecipitation; C1 (control 1), immunoprecipitation with protein A-Sepharose, lysis buffer, and specific antibody only; C2 (control 2), immunoprecipitation with protein A-Sepharose, whole-cell lysates, and preimmune rabbit serum.

### Enzastaurin inhibits MM-cell growth

We next examined the impact of PKC inhibition on MM-cell growth, survival, and migration. Enzastaurin induced marked dose-dependent growth inhibition in all MM cell lines investigated including MM.1S, MM.1R, RPMI 8226 (RPMI), RPMI-Dox40 (Dox40), NCI-H929, KMS-11, OPM-2, and U266 (Figure 3A).  $IC_{50}$  ranged from 0.6 to 1.6  $\mu$ M, except for RPMI8226 (with an  $IC_{50}$  of 4  $\mu$ M), which has markedly lower overall PKC expression than the other cell lines (Table S1). Importantly, enzastaurin also induced growth inhibition of (CD138<sup>+</sup>) MM cells isolated from 3 patients with multidrug-resistant progressive disease (Figure 3B).

### Enzastaurin inhibits MM-cell growth triggered by BMSCs

In addition to the autocrine/paracrine effects mediated by growth factors and cytokines within the MM BM microenvironment, direct MM-BMSC contact also triggers tumor-cell growth. Importantly, enzastaurin inhibited both MM.1S adhesion to BMSCs (Figure 3C) and cell growth (Figure 3D) in a BMSC-MM-cell coculture system. Moreover, enzastaurin similarly inhibited growth of CD138<sup>+</sup> MM cells isolated from a multidrug-resistant patient with clinically progressive disease (Figure 3E). Taken together, these data demonstrate that enzastaurin inhibits MM-cell growth in MM cells alone and when cocultured with BMSCs.

### Enzastaurin induces MM-cell apoptosis

We next sought to evaluate whether enzastaurin induces MM-cell apoptosis. Due to its self-fluorescence within the propidium iodide spectrum, we stained cells separately with annexin V-FITC and SYTOX green nucleic acid stain. Our data demonstrate that enzastaurin induces 55% apoptosis in MM.1S cells after 48 hours (data not shown). Moreover, MTT assays show dose-dependent enzastaurin-induced cytotoxicity in MM cell lines, but not in PBMCs isolated from 3 healthy donors (Figure 4A). Consistent with these data, protein profiling in enzastaurin-treated MM cells shows decreased phosphorylation of Akt, GSK3 $\beta$ , and cMyc as well as down-regulation of Mcl-1, but not Bcl-2 and Bcl-XL, protein expression. In addition, our data show cleavage of caspase-8, caspase-3, and PARP, but not of caspase-9 (Figure 4B). Taken together, these data confirm that enzastaurin triggers MM-cell apoptosis.

### Enzastaurin inhibits MM-cell migration

Increased microvessel density and tumor-cell expansion within the BM microenvironment, as well as tumor-cell egress into the peripheral blood, are indicators of MM progression. PKC activity is associated with VEGF- as well as IGF-1-induced endothelial and MM-cell migration.<sup>35</sup> Our data show that enzastaurin markedly

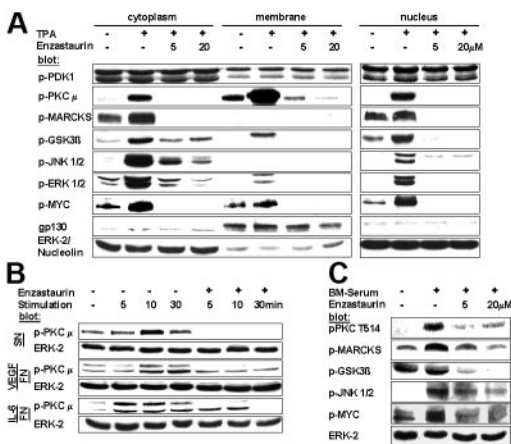


**Figure 2. Enzastaurin specifically inhibits phosphorylation of signaling molecules downstream of PKC.** (A) Enzastaurin specifically inhibits TPA-triggered phosphorylation of signaling molecules downstream of PKC. MM.1S cells were processed as described in Figure 1A and immunoblots of cytosolic, membrane, and nuclear fractions were probed with indicated antibodies. (B) Enzastaurin inhibits PKC signaling sequelae in MM cells triggered by BMSC-secreted growth factors and cytokines, as well as costimulation with the extracellular matrix protein fibronectin together with IL-6 or VEGF. Enzastaurin-treated (3 hours) or untreated MM.1S cells were stimulated with conditioned medium from the BMSC line HS-5 (supernatant [SN]), with both VEGF (100 ng/mL) and fibronectin (10 μg/mL; VEGF/FN), or with IL-6 (50 ng/mL) and fibronectin (10 μg/mL; IL-6/FN). Immunoblots were probed with indicated antibodies. (C) Enzastaurin inhibits PKC signaling sequelae in MM cells triggered by MM patient serum (BM-serum). Enzastaurin-treated (3 hours) or untreated MM.1S cells were stimulated with serum from MM patient BM. Immunoblots were probed with indicated antibodies.

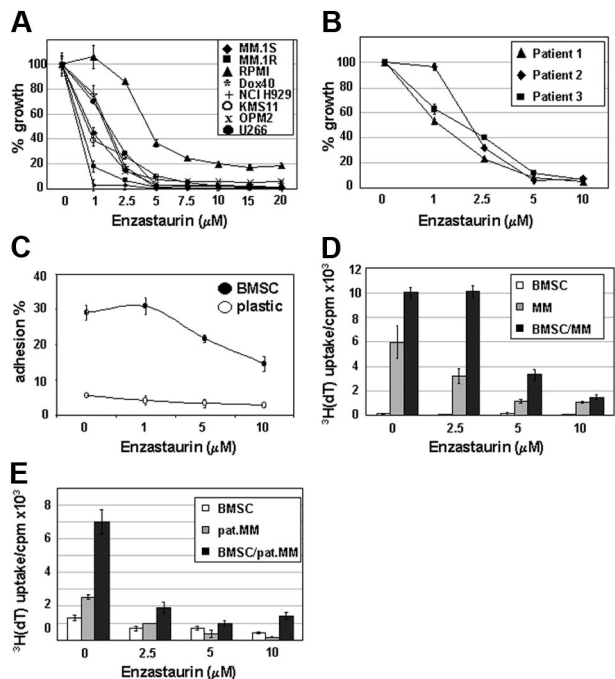


**Figure 3. Enzastaurin inhibits MM-cell growth.** (A-B) Dose-related effects of enzastaurin on proliferation of indicated MM cell lines (A) and patient cells (B). Cells were cultured with indicated concentrations of enzastaurin. Uptake of  $^3\text{H}$ -thymidine was measured during the last 10 hours of 48-hour cultures. (C) Enzastaurin decreases MM-cell adhesion to BMSCs. Spontaneous adherence of enzastaurin-treated and untreated MM cells to BMSCs was measured using calcein-AM. (D-E) Enzastaurin inhibits proliferation of MM cells adherent to BMSCs. MM.1S cells (MM; D) or CD138<sup>+</sup> MM cells (pat. MM) isolated from a multidrug-resistant patient with clinically progressive disease (E) were cultured with or without BMSCs. Enzastaurin was added in the indicated concentrations, and proliferation was measured using  $^3\text{H}$ -thymidine uptake. Data shown are the mean  $\pm$  SD of experiments performed in quadruplicate.

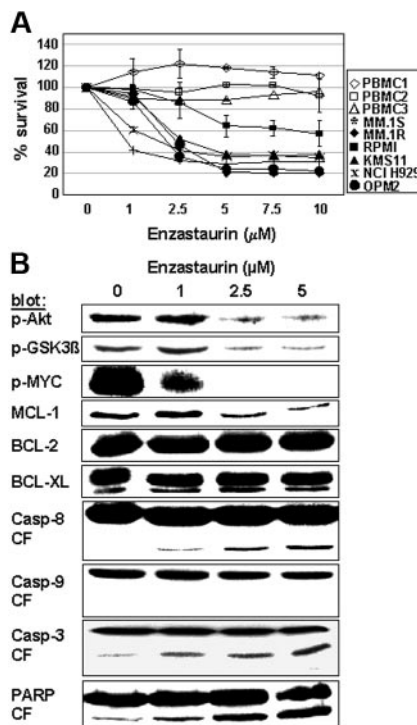


**Figure 4. Enzastaurin induces MM-cell apoptosis.** (A) Dose-related effects of enzastaurin on survival of MM cell lines and healthy donors. PBMC indicates peripheral blood mononuclear cell. MTT cleavage was measured during the last 4 hours of 48-hour cultures. (B) Protein profiling of MM cells exposed to enzastaurin. MM.1S cells were exposed to increasing concentrations of enzastaurin, followed by immunoblot analysis of the lysates with indicated antibodies.

down-regulates MM-cell adhesion to the extracellular matrix protein fibronectin (Figure 5A). Moreover, enzastaurin abrogates VEGF-triggered MM-cell migration on fibronectin as well as IGF-1-induced MM-cell migration (Figure 5B).

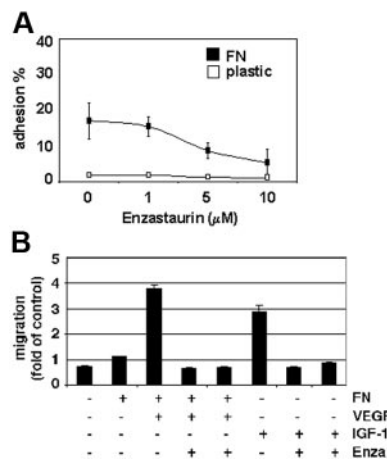


**Figure 5. Enzastaurin inhibits MM-cell adhesion to fibronectin as well as VEGF- and IGF-1-triggered MM-cell migration.** (A) Enzastaurin decreases MM-cell adhesion to fibronectin. Spontaneous adherence of enzastaurin-treated and untreated MM cells to fibronectin (20 μg/mL) was measured using calcein-AM. The results are representative of 3 independent experiments performed in quadruplicate. (B) Enzastaurin abrogates VEGF- and IGF-1-triggered MM-cell migration. Growth factor-deprived enzastaurin-treated or untreated MM.1S cells were plated on either a fibronectin-coated or noncoated membrane (8 μm pore size) in a Boyden modified chamber and stimulated with VEGF or IGF-1, respectively. Cells in the lower chamber were counted with a Coulter counter ZBII. The results shown are representative of 3 independent experiments.

### Enzastaurin has synergistic cytotoxicity with bortezomib, lenalidomide, and melphalan

Combined therapies can often enhance growth inhibition and cytotoxicity, overcome drug resistance, and avoid side effects. We therefore next investigated whether combinations of enzastaurin with novel (bortezomib and lenalidomide), or conventional (melphalan) therapies enhanced growth inhibition and cytotoxicity. Specifically, low-dose enzastaurin (0.5 and 1 nM) was combined with melphalan (0.5 and 2  $\mu$ M), lenalidomide (0.5 and 2  $\mu$ M), and bortezomib (0.5 and 2 nM), at concentrations below their in vitro IC<sub>50</sub> values (8  $\mu$ M, 5  $\mu$ M, and 5 nM, respectively). Equivalent plasma concentrations are easily achievable in MM patients.<sup>41-43</sup> Isobologram analysis of thymidine uptake demonstrated marked synergistic growth inhibition of low-dose enzastaurin and bortezomib (combination index > 0.5) and moderate synergistic (combination index, 0.7-0.9) or additive (combination index, 0.9-1.1) effects in combination with lenalidomide or melphalan, respectively (Table 1). Moreover, inhibition of survival achieved with low-dose single agent bortezomib, lenalidomide, and melphalan was markedly enhanced when given in combination with low-dose enzastaurin (Figure 6). Taken together, these results provide the framework for combination clinical trials to increase therapeutic efficacy and reduce toxicity.

### Enzastaurin blocks angiogenesis and MM-cell growth triggered by endothelial-cell adhesion

PKC activation induces endothelial-cell proliferation and migration, thereby inducing endothelial tube formation.<sup>44</sup> Importantly, enzastaurin induced marked antiangiogenic activity in the rat corneal micropocket assay and decreased microvessel density in human tumor xenografts including human breast cancer, ovarian cancer, small-cell lung cancer, colon cancer, hepatocellular cancer, gastric cancer, and glioblastoma multiforme.<sup>45</sup> Consistent with these data, our results showed marked dose-dependent in vitro down-regulation of endothelial-cell growth (Figure 7A) and tubule formation (Figure 7B) triggered by enzastaurin. Moreover, enzastaurin, similar to the PKC inhibitor bisindolylmaleimide (BIM) I,

**Table 1. Low-dose enzastaurin sensitizes MM cells to low-dose bortezomib, lenalidomide, and melphalan**

Drug dosage	Enzastaurin	FA	CI
<b>Bortezomib</b>			
0.5	0.5	0.556	0.477
1	0.5	0.621	0.409
0.5	1	0.7514	0.521
1	1	0.7988	0.45
<b>Lenalidomide</b>			
0.5	0.5	0.299	0.812
2	0.5	0.337	0.825
0.5	1	0.4828	0.98
2	1	0.5182	0.915
<b>Melphalan</b>			
0.5	0.5	0.366	0.831
2	0.5	0.58	0.815
0.5	1	0.68	0.703
2	1	0.747	0.766

Enzastaurin-treated (0.5 and 1  $\mu$ M) or untreated MM. 1S cells were exposed to bortezomib (0.5 and 1 nM), lenalidomide (0.5 and 2 nM), and melphalan (0.5 and 2  $\mu$ M). Proliferation was measured using [<sup>3</sup>H]-thymidine uptake during the last 10 hours of 48-hour cultures. FA indicates the fraction of cells with growth affected in drug-treated versus untreated cells. CI indicates the combination index. CI < 1 synergism, CI = 0.9-1.1 additive effects. The results shown are representative of 3 independent experiments performed in quadruplicate.

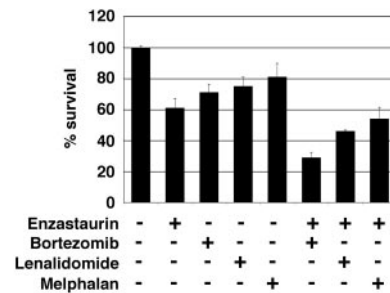


**Figure 6. Low-dose enzastaurin enhances cytotoxicity of low-dose bortezomib, lenalidomide, and melphalan.** Enzastaurin-treated (1  $\mu$ M) or untreated MM. 1S cells were exposed to bortezomib (1 nM), lenalidomide (2  $\mu$ M), and melphalan (2  $\mu$ M). MTT cleavage was measured during the last 4 hours of 48-hour cultures. Values represent the mean  $\pm$  SD absorbance of quadruplicate cultures.

abrogated TPA-induced Thr-514 and Ser-660 phosphorylation (Figure 7C, upper 2 panels), as well as subsequent activation of downstream signaling molecules including MARCKS, PKC $\mu$ /PKD, GSK3 $\beta$ , JNK1/2, ERK1/2, c-Myc, and S6 (Figure 7C). Similar to BMSCs, MM-cell growth is stimulated when bound to endothelial cells. Importantly, our results demonstrate marked enzastaurin-induced inhibition of cell growth in both the endothelial cell-MM.1S, as well as the endothelial cell-patient MM cell, coculture systems (Figure 7D).

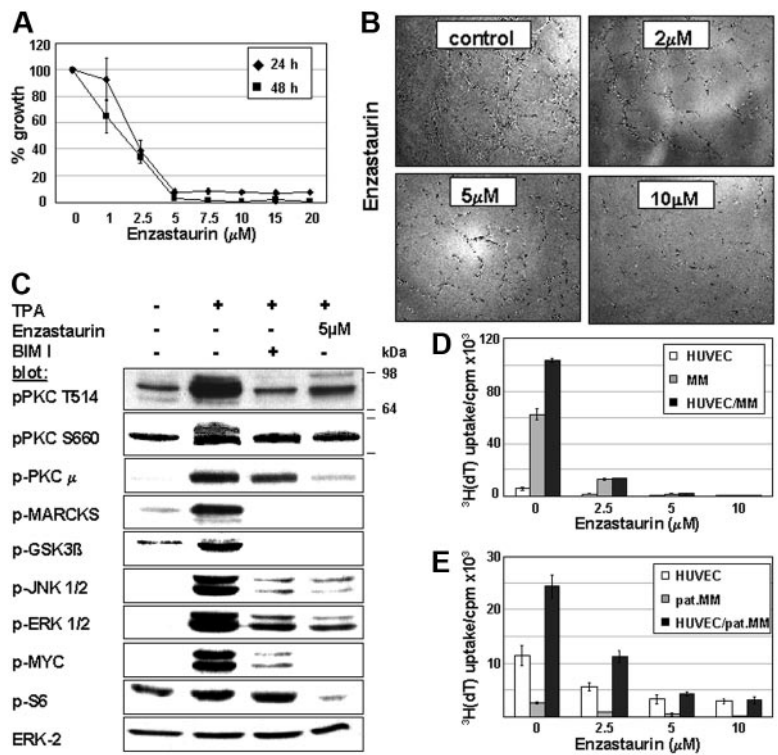
### Enzastaurin markedly decreases tumor growth in a xenograft mouse model of human MM

Having demonstrated effects of enzastaurin on both MM cells and endothelial cells in vitro, we next sought to assess the in vivo efficacy of enzastaurin using a mouse model of human MM. Immune-deficient beige-nude-xid (BNX) mice were given subcutaneous inoculations into the flank with  $3 \times 10^7$  MM.1S cells. When the tumors reached a palpable size, mice were treated with 30 mg/kg enzastaurin administered twice daily by oral gavage over an 8-week period. Tumor growth in treated mice was significantly delayed compared to the control group (Figure 8A). However, tumors rapidly regrew after cessation of treatment. Using Kaplan-Meier and log-rank analysis, the mean overall survival (OS) was 23 days (95% CI, 13-52 days) in the control cohort versus 77 days (95% CI, 50 to > 200 days) in the treatment group (Figure 8B). Statistically significant prolongation in mean OS was observed in treated animals compared with control mice ( $P = .002$ ). Importantly, treatment with either the vehicle alone or enzastaurin did not affect body weight (Figure 8C). Large areas of cells with condensed nuclei were seen in hematoxylin and eosin stains of enzastaurin-treated tumors, consistent with tumor-cell apoptosis or necrosis (Figure 8D). Angiogenesis was markedly reduced within tumors of enzastaurin-treated versus nontreated mice, as evidenced by CD31 staining (Figure 8E). Finally, TUNEL assays on tumor sections from treated versus control mice showed significantly increased apoptosis (Figure 8F). Taken together, these results demonstrate that enzastaurin triggers in vivo inhibition of tumor growth, decreased angiogenesis, and increased MM-cell apoptosis, associated with prolongation of host survival.

## Discussion

PKC serves as the major cellular receptor for the powerful tumor-promoting phorbol esters (eg, TPA).<sup>8-11</sup> Moreover, members

**Figure 7. Enzastaurin blocks TPA-induced endothelial-cell signaling pathways and MM-cell growth triggered by endothelial-cell adhesion.** (A) Dose-related effects of enzastaurin on endothelial-cell proliferation. HUVECs were cultured with indicated concentrations of enzastaurin. Proliferation was measured using [<sup>3</sup>H]-thymidine uptake during the last 8 hours of 24-hour and 48-hour cultures. (B) Enzastaurin inhibits endothelial tubule formation. Endothelial-cell suspensions were premixed with different concentrations of enzastaurin in EGM-2 and added on top of the ECMatrix. Tubule formation was assessed using an inverted light microscope at ×4 and ×10 magnification. Photographs are representative of each group and 3 independent experiments. (C) Enzastaurin specifically inhibits homologous Thr-514 and Ser-660 residue phosphorylation of PKC isoforms and downstream signaling molecules in endothelial cells. HUVECs were treated with enzastaurin (3 hours, 5 μM) or bisindolylmaleimide (BIM I) or left untreated. After stimulation with TPA (200 nM, 20 minutes), immunoblot analysis was performed with indicated antibodies. (D-E) Enzastaurin inhibits proliferation of MM cells adherent to endothelial cells. MM.1S cells (MM; D or CD138<sup>+</sup> MM cells (pat. MM) isolated from a multidrug-resistant patient with clinically progressive disease (E) were cultured with or without HUVECs. Enzastaurin was added in the indicated concentrations, and proliferation was measured using [<sup>3</sup>H]-thymidine uptake. Data shown are the mean ±SD of experiments performed in quadruplicate.



of the PKC family have been implicated in pathogenesis of both solid as well as hematologic malignancies. PKC therefore represents an attractive and promising therapeutic target. However, due to the many isoforms and their cell-specific functions, thorough

preclinical and clinical evaluation is needed assess the therapeutic potential of PKC inhibitors in various cancers. Specifically, although implicated in MM pathogenesis, the therapeutic value of targeting PKC signaling sequelae in MM is to date unknown.

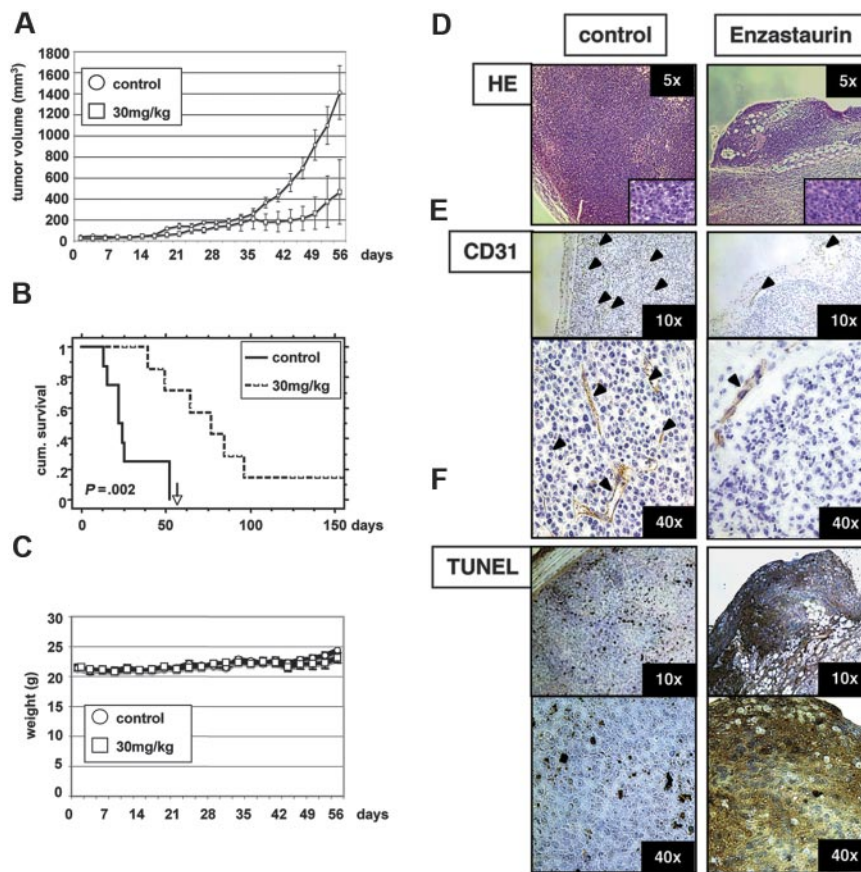


**Figure 8. Low-dose enzastaurin markedly decreases tumor growth and angiogenesis in a xenograft mouse model.** Beige-nude Xid mice were given subcutaneous inoculations in the right flank with  $3 \times 10^7$  MM.1S cells. Treatment by oral gavage (vehicle alone or 30 mg/kg enzastaurin twice daily) was started when tumors were measurable. (A) Tumor burden was measured every alternate day using a caliper. Tumor volume is presented as means ± SE. (B) Survival was evaluated using Kaplan-Meier curves and log-rank analysis. (C) Body weight was evaluated 3 times a week. (D-F) Representative microscopic images of tumor sections are shown stained with hematoxylin and eosin (D), CD31 (E), and TUNEL (F).

Here we investigated the cytotoxicity of the orally available, small-molecule PKC inhibitor enzastaurin against MM. Promising preclinical and early clinical efficacy data have already led to a phase 3 clinical trial in DLBCL and early-phase clinical trials are ongoing in solid as well as hematologic malignancies. Due to our expression profiling studies in MM cells, we focused our present studies on PKC $\alpha$ , PKC $\beta$ , PKC $\delta$ , and PKC $\epsilon$ . We demonstrate that enzastaurin specifically targets TPA- and microenvironment-induced PKC activity, without modulating stimuli-induced PKC membrane recruitment. Interestingly, our data additionally indicate that enzastaurin induced sustained PKC binding to the plasma-cell membrane, thereby blocking the release of activated PKC into the cytoplasm and subsequent activation of downstream molecules. Enzastaurin also induced marked inhibition of PKC isoform phosphorylation within the nucleus, consistent with previous data indicating an important role for nuclear PKC isoforms in the regulation of cell growth, differentiation, neoplastic transformation, and apoptosis.<sup>46</sup> Our ongoing studies are further evaluating the role of PKC isoforms in MM by investigating their membrane interaction, cellular sublocalization, specific protein interactions, and mutual regulation. Importantly, although our studies focused on PKC isoforms with overall high expression levels (eg, PKC $\alpha$ , PKC $\beta$ , PKC $\delta$ , and PKC $\epsilon$ ), we have not excluded a potential pathophysiologic role for those PKC isoforms with low expression levels and therefore are including them into our studies.

Functionally, enzastaurin strongly inhibits growth and survival of a broad range of MM cell lines and patient MM cells, including those with the prognostic adverse t(4;14) translocation, including NCI-H929 (with wild-type FGFR3 overexpression), OPM-2 (with FGFR3 mutation K650E), and KMS-11 (with FGFR3 mutation Y373C). In contrast, PKC412 (N-benzoyl-staurosporine; Novartis Pharma, Basel, Switzerland), initially also developed as a PKC inhibitor, showed marked efficacy only in MM cells overexpressing wild-type FGFR3 or FGFR3 mutants.<sup>47</sup> Importantly, marked up-regulation of PKC $\beta$  was reported in MM patients with the t(4;14)(p16;q32) translocation.<sup>36,37</sup> Ongoing studies are investigating whether PKC $\beta$  up-regulation within this patient group is directly linked to overexpression of wild-type FGFR3 and MMSET and subsequent FGFR3-activating mutations and whether these effects can be modulated by enzastaurin. Molecular mechanisms by which PKC isoforms regulate cell growth and survival are still elusive. Studies to delineate downstream mechanisms by which the PKC isoforms  $\alpha$ ,  $\beta$ ,  $\delta$ ,  $\epsilon$ -PKC $\mu$ /MARCKS/JNK/ERK/c-Myc pathway mediate TPA-, serum-, VEGF/FN-, IL-6/FN-triggered growth and survival in MM cells are ongoing. Although enzastaurin inhibits GSK3 $\beta$  phosphorylation in PBMCs,<sup>25</sup> our data show no inhibition of cell survival, suggesting that MM-specific activity of enzastaurin may either be GSK3 $\beta$ -independent or a tumor cell-specific effect. Importantly, inhibition of GSK3 $\beta$  phosphorylation may serve as a biomarker for enzastaurin activity.<sup>25</sup>

Besides MM proliferation and survival, enzastaurin blocks VEGF- and IGF-1-triggered MM-cell migration, angiogenesis, as

well as MM-cell growth triggered by MM-endothelial-cell binding. Recent advances in MM therapy have demonstrated advantages of combination therapy. Moreover, to increase antitumor effects, recent reports strongly suggest the use of PKC inhibitors together with chemotherapeutics or targeted therapies. Indeed, our *in vitro* studies in MM show synergistic effects for enzastaurin with the proteasome inhibitor bortezomib and moderate synergistic or additive effects when combined with melphalan or lenalidomide. Finally, oral dosing of enzastaurin in a MM xenograft mouse model markedly decreases tumor burden directly, via inhibition of MM-cell proliferation and induction of apoptosis, and indirectly, via inhibition of tumor angiogenesis.

In summary, these *in vitro* and *in vivo* data support the pivotal role for members of the PKC family in MM pathogenesis and provide the framework for protocol evaluation of the novel, orally available PKC inhibitor enzastaurin, either alone or in combination with bortezomib, lenalidomide, or melphalan, to enhance therapeutic efficacy, reduce adverse side effects, and improve outcome in patients with MM.

## Acknowledgments

This work was supported by a MMRF Senior Research grant award (K.P.); a grant from the Fritz-Thyssen Foundation (M.S. Raab); National Institutes of Health grants RO CA50947, PO-1 CA78378, and P50 CA100707; and the Doris Duke Distinguished Clinical Research Scientist Award (K.C.A.).

We thank F. Abtahi for technical assistance and Drs A. Cardoso and M. Tavares for providing HUVECs. The authors further acknowledge the contribution of Dr P.G. Richardson and Dr R. Schlossman, as well as the patients, nursing staff, and clinical research coordinators of the Jerome Lipper Multiple Myeloma Center/Dana-Farber Cancer Institute for their help in providing primary tumor specimens for this study.

## Authorship

Contribution: K.P. designed, performed, and analyzed research and wrote the manuscript; M.S.R. designed, performed and analyzed research; J.Z., D.M., and I.B. performed research; and Y.T.T., B.K.L., N.M., T.H., D.C., and K.C.A. analyzed data.

Conflict-of-interest disclosure: B.K.L. is an employee of Eli Lilly and Company.

K.P. and M.S.R. contributed equally to the study.

Correspondence: Klaus Podar and Kenneth C. Anderson, Dana-Farber Cancer Institute, Department of Medical Oncology, Jerome Lipper Multiple Myeloma Center, 44 Binney St, Boston, MA 02115; e-mail: kenneth\_anderson@dfci.harvard.edu and klaus\_podar@dfci.harvard.edu.

## References

- Nishizuka Y. The Albert Lasker Medical Awards. The family of protein kinase C for signal transduction. *JAMA*. 1989;262:1826-1833.
- Nishizuka Y. Studies and perspectives of protein kinase C. *Science*. 1986;233:305-312.
- Asaoka Y, Nakamura S, Yoshida K, Nishizuka Y. Protein kinase C, calcium and phospholipid degradation. *Trends Biochem Sci*. 1992;17:414-417.
- Dekker LV, Parker PJ. Protein kinase C—a question of specificity. *Trends Biochem Sci*. 1994;19:73-77.
- Nishizuka Y. Protein kinase C and lipid signaling for sustained cellular responses. *FASEB J*. 1995;9:484-496.
- Newton AC. Protein kinase C: structure, function, and regulation. *J Biol Chem*. 1995;270:28495-28498.
- Newton AC. Regulation of protein kinase C. *Curr Opin Cell Biol*. 1997;9:161-167.
- Berenblum I. The mechanism of carcinogenesis: a study of the significance of carcinogenic action and related phenomena. *Cancer Res*. 1941;1:807-814.
- Castagna M, Takai Y, Kaibuchi K, Sano K, Kikkawa U, Nishizuka Y. Direct activation of calcium-activated, phospholipid-dependent protein kinase by tumor-promoting phorbol esters. *J Biol Chem*. 1982;257:7847-7851.
- Nishizuka Y. The role of protein kinase C in cell



- surface signal transduction and tumour promotion. *Nature*. 1984;308:693-698.
11. Nishizuka Y. Discovery and prospect of protein kinase C research: epilogue. *J Biochem (Tokyo)*. 2003;133:155-158.
  12. O'Brian C, Vogel VG, Singletary SE, Ward NE. Elevated protein kinase C expression in human breast tumor biopsies relative to normal breast tissue. *Cancer Res*. 1989;49:3215-3217.
  13. Takenaga K, Takahashi K. Effects of 12-O-tetradecanoylphorbol-13-acetate on adhesiveness and lung-colonizing ability of Lewis lung carcinoma cells. *Cancer Res*. 1986;46:375-380.
  14. Schwartz GK, Jiang J, Kelsen D, Albino AP. Protein kinase C: a novel target for inhibiting gastric cancer cell invasion. *J Natl Cancer Inst*. 1993;85:402-407.
  15. Gokmen-Polar Y, Murray NR, Velasco MA, Gatalica Z, Fields AP. Elevated protein kinase C beta11 is an early promotive event in colon carcinogenesis. *Cancer Res*. 2001;61:1375-1381.
  16. da Rocha AB, Mans DR, Regner A, Schwartsmann G. Targeting protein kinase C: new therapeutic opportunities against high-grade malignant gliomas? *Oncologist*. 2002;7:17-33.
  17. Dean N, McKay R, Miraglia L, et al. Inhibition of growth of human tumor cell lines in nude mice by an antisense of oligonucleotide inhibitor of protein kinase C-alpha expression. *Cancer Res*. 1996;56:3499-3507.
  18. Shipp MA, Ross KN, Tamayo P, et al. Diffuse large B-cell lymphoma outcome prediction by gene-expression profiling and supervised machine learning. *Nat Med*. 2002;8:68-74.
  19. Hans CP, Weisenburger DD, Greiner TC, et al. Expression of PKC-beta or cyclin D2 predicts for inferior survival in diffuse large B-cell lymphoma. *Mod Pathol*. 2005;18:1377-1384.
  20. Felli MP, Vacca A, Calce A, et al. PKC theta mediates pre-TCR signaling and contributes to Notch3-induced T-cell leukemia. *Oncogene*. 2005;24:992-1000.
  21. Gorelik G, Barreiro Arcos ML, Klecha AJ, Cremaschi GA. Differential expression of protein kinase C isoenzymes related to high nitric oxide synthase activity in a T lymphoma cell line. *Biochim Biophys Acta*. 2002;1588:179-188.
  22. Villalba M, Kasibhatla S, Genestier L, Mahboubi A, Green DR, Altman A. Protein kinase C theta co-operates with calcineurin to induce Fas ligand expression during activation-induced T cell death. *J Immunol*. 1999;163:5813-5819.
  23. Goekjian PG, Jirousek MR. Protein kinase C inhibitors as novel anticancer drugs. *Expert Opin Investig Drugs*. 2001;10:2117-2140.
  24. Taylor CJ, Motamed K, Lilly B. Protein kinase C and downstream signaling pathways in a three-dimensional model of phorbol ester-induced angiogenesis. *Angiogenesis*. 2006;9:39-51.
  25. Graff JR, McNulty AM, Hanna KR, et al. The protein kinase C beta-selective inhibitor, Enzastaurin (LY317615.HCl), suppresses signaling through the AKT pathway, induces apoptosis, and suppresses growth of human colon cancer and glioblastoma xenografts. *Cancer Res*. 2005;65:7462-7469.
  26. Keyes KA, Mann L, Sherman M, et al. LY317615 decreases plasma VEGF levels in human tumor xenograft-bearing mice. *Cancer Chemother Pharmacol*. 2004;53:133-140.
  27. Green LJ, Marder P, Ray C, et al. Development and validation of a drug activity biomarker that shows target inhibition in cancer patients receiving enzastaurin, a novel protein kinase C-beta inhibitor. *Clin Cancer Res*. 2006;12:3408-3415.
  28. Herbst RS, Thornton DE, Kies MS. Phase 1 study of LY317615, a protein kinase C beta inhibitor. *Proc ASCO*. 2002;21:82a.
  29. Parant MR, Klein B, Vial H. Abnormal behavior of protein kinase C in the human myeloma cell line, RPM1 8226. *FEBS Lett*. 1990;269:331-335.
  30. Ni H, Ergin M, Tibudan SS, Denning MF, Izban KF, Alkan S. Protein kinase C-delta is commonly expressed in multiple myeloma cells and its downregulation by rottlerin causes apoptosis. *Br J Haematol*. 2003;121:849-856.
  31. Thabard W, Collette M, Bataille R, Amiot M. Protein kinase C delta and eta isoenzymes control the shedding of the interleukin 6 receptor alpha in myeloma cells. *Biochem J*. 2001;358:193-200.
  32. Podar K, Tai YT, Lin BK, et al. Vascular endothelial growth factor-induced migration of multiple myeloma cells is associated with beta 1 integrin- and phosphatidylinositol 3-kinase-dependent PKC alpha activation. *J Biol Chem*. 2002;277:7875-7881.
  33. Qiang YW, Walsh K, Yao L, et al. Wnts induce migration and invasion of myeloma plasma cells. *Blood*. 2005;106:1786-1793.
  34. Chauhan D, Pandey P, Ogata A, et al. Cytochrome c-dependent and -independent induction of apoptosis in multiple myeloma cells. *J Biol Chem*. 1997;272:29995-29997.
  35. Podar K, Anderson KC. The pathophysiologic role of VEGF in hematologic malignancies: therapeutic implications. *Blood*. 2005;105:1383-1395.
  36. Bergsagel PL, Kuehl WM, Zhan F, Sawyer J, Barlogie B, Shaughnessy J Jr. Cyclin D dysregulation: an early and unifying pathogenic event in multiple myeloma. *Blood*. 2005;106:296-303.
  37. Dring AM, Davies FE, Fenton JA, et al. A global expression-based analysis of the consequences of the t(4;14) translocation in myeloma. *Clin Cancer Res*. 2004;10:5692-5701.
  38. Podar K, Shringarpure R, Tai YT, et al. Caveolin-1 is required for vascular endothelial growth factor-triggered multiple myeloma cell migration and is targeted by bortezomib. *Cancer Res*. 2004;64:7500-7506.
  39. Chauhan D, Catley L, Hideshima T, et al. 2-Methoxyestradiol overcomes drug resistance in multiple myeloma cells. *Blood*. 2002;100:2187-2194.
  40. Rizvi MA, Ghias K, Davies KM, et al. Enzastaurin (LY317615), a protein kinase C beta inhibitor, inhibits the AKT pathway and induces apoptosis in multiple myeloma cell lines. *Mol Cancer Ther*. 2006;5:1783-1789.
  41. Kaufman JL, Lonial S. Proteasome inhibition: novel therapy for multiple myeloma. *Onkologie*. 2006;29:162-168.
  42. Kumar S, Rajkumar SV. Thalidomide and lenalidomide in the treatment of multiple myeloma. *Eur J Cancer*. 2006;42:1612-1622.
  43. Kyle RA, Rajkumar SV. Multiple myeloma. *N Engl J Med*. 2004;351:1860-1873.
  44. Montesano R, Orci L. Tumor-promoting phorbol esters induce angiogenesis in vitro. *Cell*. 1985;42:469-477.
  45. Teicher BA, Alvarez E, Menon K, et al. Antiangiogenic effects of a protein kinase C beta-selective small molecule. *Cancer Chemother Pharmacol*. 2002;49:69-77.
  46. Martelli AM, Evangelisti C, Nyakern M, Manzoli FA. Nuclear protein kinase C. *Biochim Biophys Acta*. 2006;1761:542-551.
  47. Chen J, Lee BH, Williams IR, et al. FGFR3 as a therapeutic target of the small molecule inhibitor PKC412 in hematopoietic malignancies. *Oncogene*. 2005;24:8259-8267.